

## Fine-Blanking Punch Edge Control by Chamfering and Plasma-Nitriding under Excessive Load Situation

Kenji Fuchiwaki<sup>1,a\*</sup> and Tatsuhiko Aizawa<sup>2,b</sup>

<sup>1</sup>183-7 Hirasawa Hadano, Kanagawa, 257-0015, Japan

<sup>2</sup>1-29-1 Nishi-Rokugo, Ota-City, Tokyo 144-0056, Japan

<sup>a\*</sup>kenji-fuchiwaki@hatanoseimitsu.co.jp, <sup>b</sup>taizawa@sic.shibaura-it.ac.jp

**Keywords:** fine blanking, punch edge shape control, plasma nitriding, less punch edge distortion.

**Abstract.** A fine blanking (FB) has grown up as a manufacturing means to fabricate the precise automotive parts from the thick sheet metals. During this net-shaping process, each part product had fully burnished surfaces through a single stroke. The punch for this FB, were highly loaded enough to distort the punch edge and to deteriorate the cost competitiveness and sustainability. A chamfered SKH51 tool steel punch was designed by controlling the chamfer widths and angles. A massively nitrogen supersaturated SKH51 punch was also prepared to investigate its effect on the suppression of punch edge distortion. AISI304 stainless steel work was used to describe the variation of punch distortion and blank qualities with increasing the number of strokes.

### Introduction

Fine blanking (FB) has been growing up as a key metal forming means to fabricate the precise automotive parts from the thick sheet metals [1]. During this net-shaping process, each part product is formed to have fully burnished surfaces through a single stroke under the narrow clearance between the outer diameter of FB-punch and the inner diameter of FB-die [2]. In addition, as depicted in Fig. 1, the work sheet metal is fixed by the FB-punch against the counter punch (CP), and, by the FB-die against the blank-holder (BH). Under this situation, the punch and die edges are subjected to severe loading. As stated in [3, 4], the normal and shear stresses concentrate at the FB-punch edges and surfaces due to the singular points in the metal flow around the edge corners. To be free from this severe FB conditions, the clearance is possible to be widened; then, the dimensional accuracy as well as the sheared surface quality deteriorate by themselves, without any treatment, the FB-punch tool life can be shortened to worse the cost-competitiveness [5, 6]. This trade-off-balancing is only saved by a new FB-punch design.

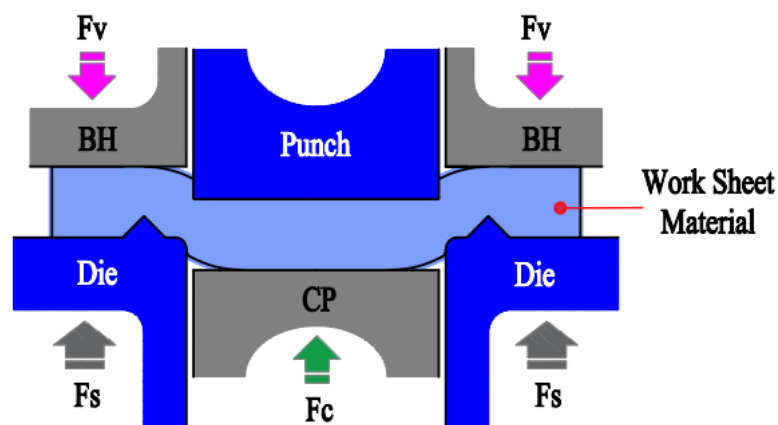


**Fig. 1.** A typical fine blanking process where the blank is fixed by the punch against counter punch (CP) and by the die against the blank-holder (BH), and, the blank holding load ( $F_v$ ), the counter load ( $F_c$ ), and, blanking load ( $F_s$ ) are applied at the same time.

In the present paper, the punch-edge chamfering and the punch surface hardening are proposed as a new FB-punch design to reduce the stress concentration at the vicinity of punch edges by controlling

the local metal flow along the chamfered punch edges and to reduce the geometric distortion of FB-punch by strengthening and hardening. In the former, the FB-punch edge profile is controlled by precise machining to have the tailored chamfer width ( $w$ ) and skew angle ( $\theta$ ). In the latter, the plasma immersion nitriding process is employed to make massive nitriding supersaturation (MNS) of FB-punch surfaces at 673 K for 14.4 ks [7, 8]. No nitride precipitates are synthesized by this MNS as stated in [8, 9]; then, no risks are embedded in the MNSed punches to initiate the fatigue cracking from the inside of punch. The homogeneous MNSed layer is formed around the FB-punch surfaces. A bare SKH51 FB-punch is employed as a reference to describe the fine blanking behavior with less geometric distortion by these two approaches and to demonstrate the FB-punch life extension without reduction of product qualities by experiments.

## Methods and Materials

### FB-Punch Design.

A new FB-punch was designed to chamfer its edges and edge-corners by controlling the chamfer width and skew angle and to make surface treatment of its head and surfaces by MNS.

In fine blanking, the punch edge geometry strongly affects burr formation and assembly accuracy. A sharp edge promotes smooth shearing and minimizes burr height, since the punch edge cross-section is directly transferred to the burr. When a rounded edge is used, the burr in the thickness direction becomes thinner and is more likely to detach and remain on the die surface, which may cause appearance defects or functional problems. Therefore, a chamfered edge was adopted instead of a rounded edge to maintain a sharp cutting interface while controlling edge deformation and suppressing burr growth in the thickness direction.

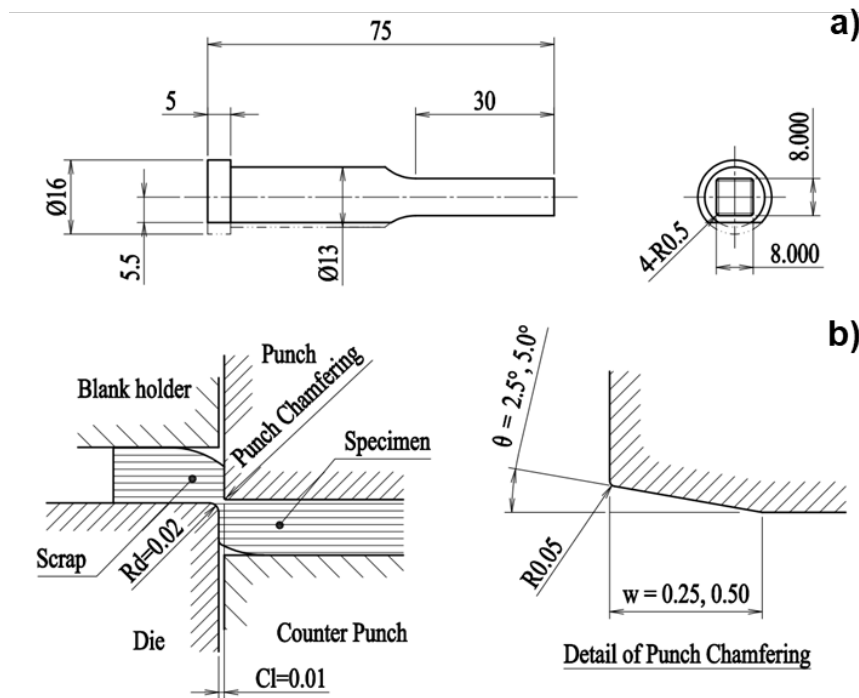


**Fig. 2.** A newly designed FB-punch. a) Geometric configuration of SKD51 FB-punch, and b) punch edge chamfering design.

### Chamfering.

A SKH51 high-speed steel punch with the hardness of 62 HRC, was commonly utilized in the following experiments with and without chamfers. As depicted in Fig. 2a, it had a square head by 8.00 mm x 8.00 mm. Its edge was chamfered to have its width of 0.25 and 0.50 mm and its skewed angle of 2.5° and 5.0°, as shown in Fig. 2b. The die was also made of SKH51. The clearance was held constant by 0.01 mm.

### Massive Nitrogen Supersaturation (MNS) Treatment.

A plasma immersion nitriding system was utilized to make MNS treatment of SKH51 high-speed steel punch. As schematically depicted in Fig. 3, the punch was placed in the hollow cathode to intensify the nitrogen ion and NH-radical densities for efficient MNS. After evacuation to the base pressure of 0.1 Pa, the nitrogen gas was introduced to the chamber; the punch was heated up in the nitrogen atmosphere at 100 Pa up to 673 K. After pre-sputtering at 673 K for 1.8 ks under the DC (Direct Current) plasma by -500 V at 60 Pa under the nitrogen gas flow, the punch was MNSed at 673 K for 16.0 ks at 60 Pa. Together with the DC-bias, RF (Radio-Frequency) voltage was applied by +250 V. The nitrogen to hydrogen gas flow rate was selected to be 100 mL/min to 20 mL/min after the plasma diagnosis through OES (Optical Emission Spectroscopy). This MNS treatment was followed by cooling down to RT under the nitrogen atmosphere.

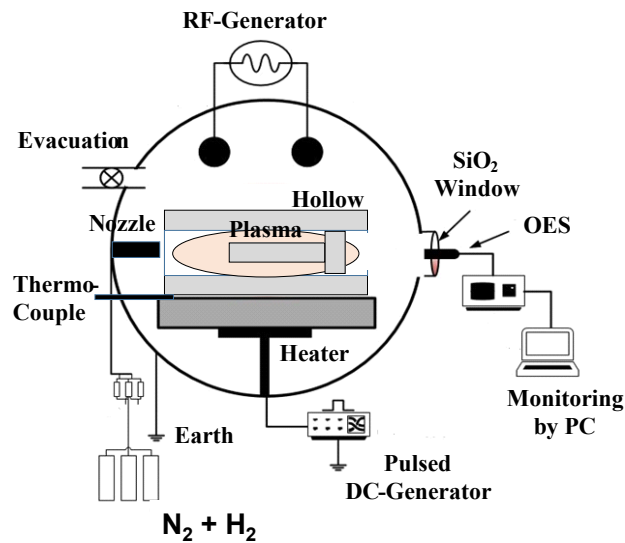


**Fig. 3.** A schematic view on the plasma immersion nitriding system for MNS treatment of SKH51 punches at 673 K.

### Measurement.

The punch edge profile at the R0.5 corner was measured by using the contact type contour profilometer at the specified number of strokes by  $N = 1, 2, 5, 10, 20$  and  $50$ , respectively. The die-roll and burr heights of blank were also measured at each  $N$  in the above.

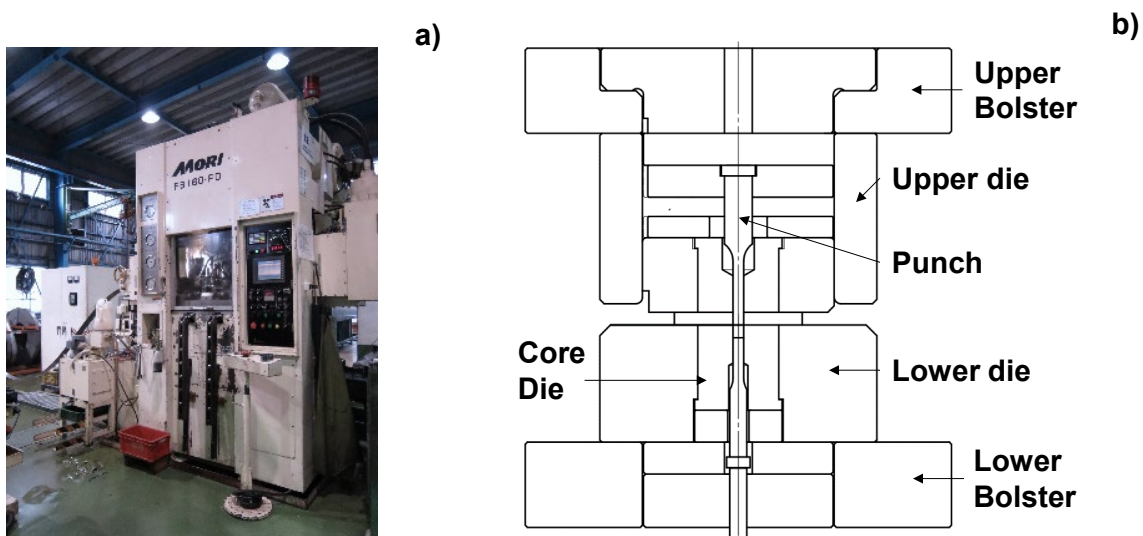


**Fig. 4.** Fine blanking experimental setup. a) Overview on the fine blanking press machine, b) die setup including the FB-punch and core-die.

### FB system.

A hydraulic press machine (FB-160FD manufactured by Mori Iron Works, Co., Ltd., Saga, Japan) was utilized in the following fine blanking experiments, as shown in Fig. 4a. The blank holding load was 80 kN, the counter load was 40 kN, and, the blanking speed was 10 mm/s. The lubricant (FBH9-HMC, Nihon Kohsakyu Co., Ltd., Tokyo, Japan) with the viscosity of 101 mm<sup>2</sup>/s was pasted onto the work sheet material.

### Materials.

#### Work Materials.

AISI304 austenitic stainless steel plate with the yield stress of 352 MPa and the tensile strength of 638 MPa was used as work material. Its thickness was 3.0 mm.

#### FB punch and die Materials.

SKH51 high-speed steel with the hardness of 62 HRC were commonly used in every case.

## Results

### Fine Blanking Behavior.

Fine blanking experiments were performed to investigate the effect of chamfering and MNS treatment of FB-punches on the abrasive wear at the punch edges with increasing the number of strokes (N).

#### Bare Punch.

A bare FB punch in Fig. 2a was used as the normal punch. As shown in Figs. 5a and 5b, the edges and edge-corners were worn out in abrasive to deteriorate the punch edge profiles only at N = 10. Figure 5c depicts the variation of edge cross-section with N. The bulging displacement or the lateral displacement advances even in the early stage of N together with the vertical displacement. This geometric distortion at N = 10 exceeds the tolerance for continuous fine blanking operations. In particular, the axial displacement, Dz, reaches Dz = 20 μm at N = 1, and, Dz = 30 μm at N = 10.

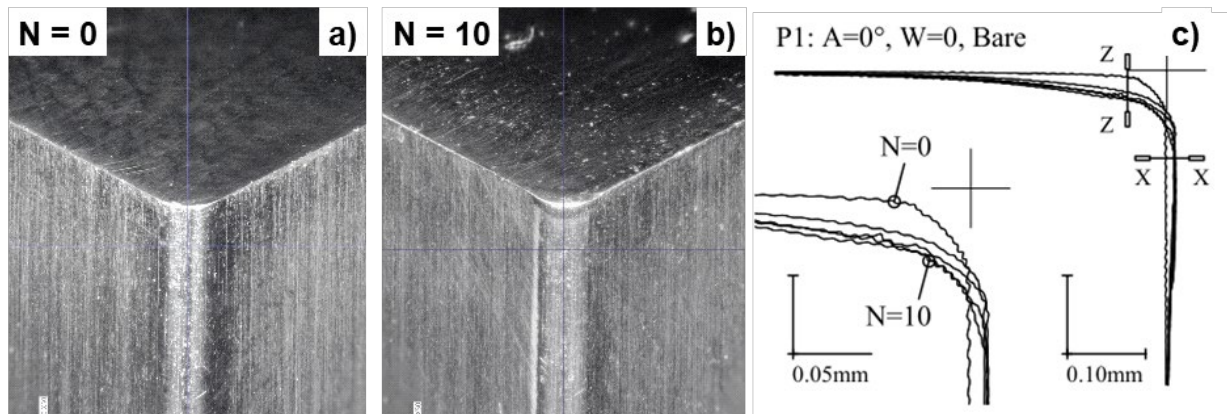


**Fig. 5.** Evolution of the wear damage at the punches with N when using the normal punch. a) Punch configuration at N = 0, b) punch configuration at N = 10, and c) variation of the edge cross-sections with N.

In application of chamfering to the edges, this Dz for the bare punch was employed as a reference to investigate the effect of chamfering width and skew angle on the geometric distortion.

#### Chamfer Width Effect.

The chamfer width was varied to be 0.25 mm and 0.5 mm. Figure 6. depicts the variation of axial displacement, Dz, at the edge-corner when the skew angle was constant by 2.5°. When w = 0.50 mm, Dz monotonically increased with N and becomes 10 μm at N = 50. On the other hand, Dz increased with N and approaches to 15 μm at N = 5. It saturates to 18 μm even increasing N to 50 when w =

0.25 mm. This revealed that the geometric distortion is controllable within the engineering tolerance when reducing the chamfer width was set to be 0.25 mm.

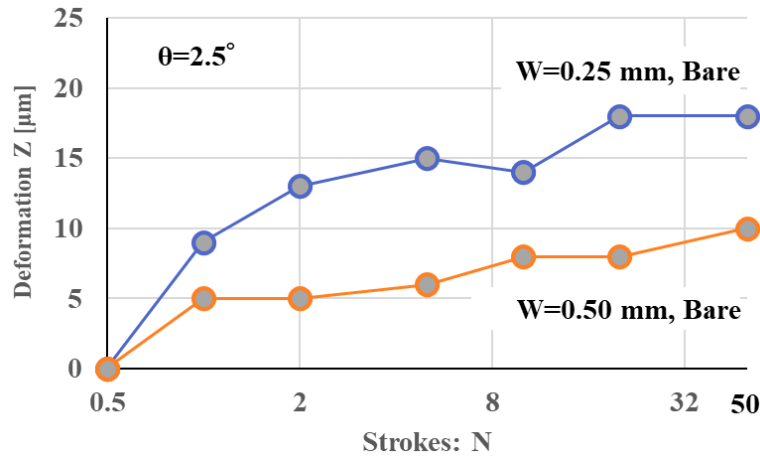


**Fig. 6.** Variation of the axial displacement at the edge corner with N for  $w = 0.25$  and  $0.50$  mm when the skew angle is constant by  $2.5^\circ$ . And bare punch surface.

#### Chamfer Skewed Angle Effect.

The chamfer skew angle  $\theta$ , also has a possibility to influence on the geometric distortion at the edges and edge-corners in the similar manner to  $w$ . Figure 7 shows the variation of  $Dz$  with N for  $\theta = 2.5^\circ$  and  $5.0^\circ$  when  $w$  is constant by  $0.25$  mm. At the beginning,  $Dz$  at  $\theta = 2.5^\circ$  is more than  $Dz$  at  $\theta = 5.0^\circ$ . After  $N = 5$ , both are nearly the same;  $Dz$  at  $\theta = 5.0^\circ$  turns to exceed  $Dz$  at  $\theta = 2.5^\circ$  when  $N = 50$ . This reveals that smaller chamfer skew angle reduces the geometric distortion at the edge corner when the chamfer width is selected to be  $0.25$  mm.

Through this parametric survey,  $w = 0.25$  mm and  $\theta = 2.5^\circ$  must be optimum to reduce the geometric distortion at the edges and edge-corners with reference to the bare punch with  $w = 0.0$  mm and  $\theta = 0.0^\circ$ .

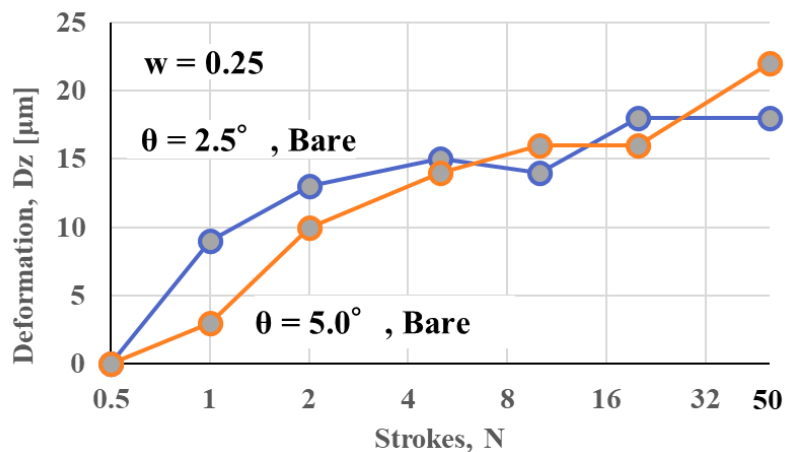


**Fig. 7.** Variation of the axial displacement at the edge-corner with N for  $\theta = 2.5^\circ$  and  $5.0^\circ$  when  $w$  is constant by  $0.25$  mm. And bare punch surface.

#### Hardening by MNS.

Reduction of punch edge displacements proves that stress concentration at the edges and edge-corners was relaxed by chamfering the edges in width and skew angle. Because of no change in the constitutive punch materials, the risk of abrasive and adhesive wears is still left as an engineering issue.

The plasma immersion nitriding system was utilized to form a massively nitrogen supersaturated layer from the punch surface to the depth of  $40\ \mu\text{m}$ . As shown in Fig. 8, the punch head and side surface were surrounded by this layer with higher nitrogen content than 1 mass%. Its average hardness reached 1400 HV. By this pretreatment, the original SKH51 punch with 62 HRC or 750 HV has a surface hardened layer with +650 HV. This surface hardening provided a way to promote the abrasive wear resistance. Nitrogen supersaturation with high nitrogen solute content also played a role to promote the adhesive wear resistance. In particular, when fine-blanking the difficult-to-forging work materials, such as austenitic stainless steels and titanium, this adhesive wear or galling exaggerate the shortage of punch life as well as the low quality of products.

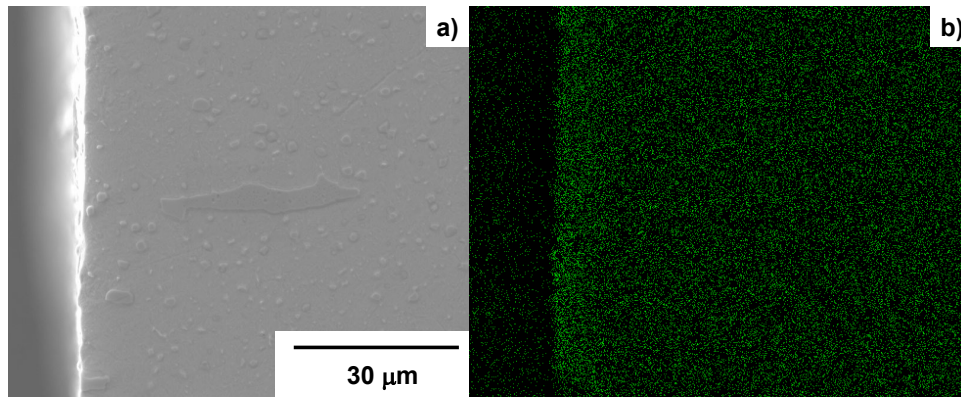


**Fig. 8.** SEM image and nitrogen mapping on the cross-section of SKH51 tool materials after massive nitrogen supersaturation.

#### Fine Blanking by Optimum-Chamfered and MNSed Punch

The chamfer width and angle were optimized to be 0.25 mm and  $2.5^\circ$ . This chamfered punch was MNSed to cover the punch by hardened layer.

#### Fine Blanking Behavior.

The punch configuration was shown in  $N = 0$  and  $N = 50$ , Figs. 9a and 9b. Although the normal and chamfered punches suffered from severe abrasive and adhesive wears, no significant wear-damages were detected at the edges and edge-corners of chamfered and MNSed punches. Figure 9c describes the variation of edge cross-sections with  $N$ . No bulging or lateral displacements were detected while the vertical displacement was suppressed to  $5\ \mu\text{m}$ . As compared to Fig. 5c, this no lateral displacement at the edges and edge-corners preserves the initial clearance between the punch outer diameter and the punch-guide inner diameter even after increasing the number of strokes. In addition, the axial displacement was less than  $5\ \mu\text{m}$  in Fig. 9c becomes much smaller than those in Figs. 6 and 7.

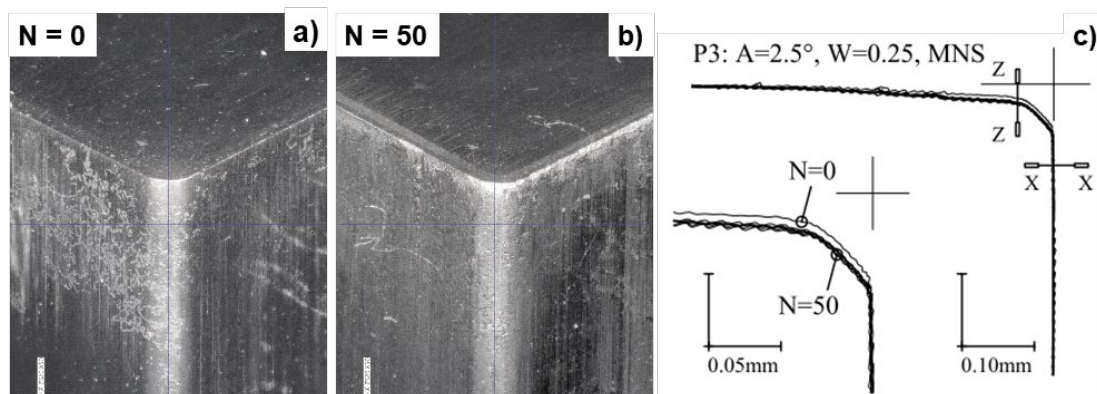


**Fig. 9.** Evolution of the wear damage at the punches with  $N$  when using the chamfered and MNSed punch. a) Punch configuration at  $N = 0$ , b) punch configuration at  $N = 10$ , and c) variation of the edge cross-sections with  $N$ .

This significant reduction of lateral and axial displacement at the punch edge cross-section proved that abrasive and adhesive wear resistance was promoted by MNS treatment.

### Quality of Blanks.

The punch displacements in the X- and Z-directions reflects on the burr and die-roll heights of sheared blanks as suggested in [10]. The die roll of blank is pushed back by shearing to leave the die-roll height at the edge corners of sheared blank. The burr of blank is also formed by local metal flow into the clearance around the edge corner. These two dimensional inaccuracies of product were measured at the specified number of strokes. Figure 10 compares the variation of the burr and die-roll heights, or Zb and Zd, with increasing N among three punches.

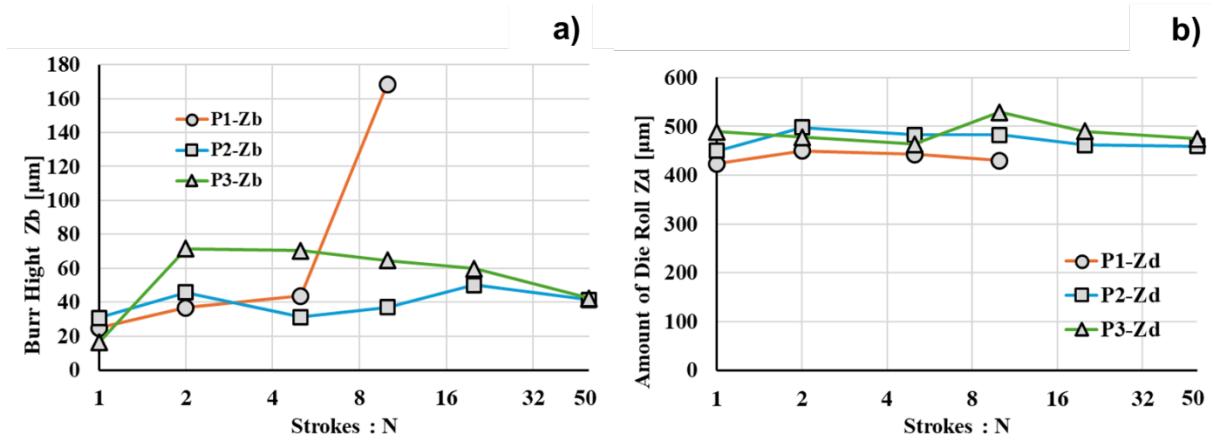


**Fig. 10.** Evolution of the burr and die-roll heights, or, Zb and Zd with increasing N when using the optimum chamfered and MNSed punches with comparison to other two punches. a) Variation of Zb with N, and, b) variation of Zd with N.

Figure 10a compared the burr height (Zb) evolution with N. Since the edges and edge-corners were worn out at  $N \sim 10$ , Zb abruptly enhanced itself for  $N > 5$  when using the normal punch. When using the chamfered punch, Zb fluctuated between 45 to 50  $\mu\text{m}$  irrespectively of N. On the other hand, when using the chamfered and MNSed punch, Zb increased to 70  $\mu\text{m}$  at  $N = 2$ ; this Zb monotonously decreased with N and  $Zb < 50 \mu\text{m}$  at  $N = 50$ . This revealed that the burr height was suppressed in the early stage of strokes by the chamfered and MNSed punch to preserve the blank quality.

The evolution of die-roll height (Zd) with N was compared among three punches in Fig. 10b. No significant difference was detected, and Zd ranged from 420 to 480  $\mu\text{m}$  for three punches.

### Discussion

In literature, many studies have been performed toward tool life extension during FB. As stated in [11-12], importance on the advanced heat treatment and coating was stressed in addition to tool-steel high qualification. Numerical simulation was utilized to make parametric survey on the effect of clearance on the metal flow during FB [13]. A very few directions to suppress the abrasive wear in FB were pointed out. In particular, no policies were proposed on the punch edge profile control and its synergetic rule with surface treatment.

After parametric survey in the present study, the chamfering width (w) and skewed angle ( $\theta$ ) had much influence on the geometric distortion. With narrowing w and  $\theta$ , the local metal flow approaches to a stream pattern with singular points at the edges and edge-corners [3], and then w and  $\theta$  must be  $w > 0.1 \text{ mm}$  or clearance and  $\theta > 1^\circ$ . On the other hand, more w than 0.5 mm, and  $\theta > 5^\circ$  deteriorate the dimensional accuracy of products. Hence, w and  $\theta$  had optimum ranges to balance the trade-off between the tool-life shortage by geometric distortion of punch edges and the dimensional accuracy of products.

Without local metal flow control around the edges and edge-corners, the hardened punch surface layer was inevitably subjected to abrasive wear by normal and shear stress concentration [3]. In order

to make full use of synergetic effect in the present method, the punch edges must be first chamfered and then MNSed to constraint the punch surface layers by hardening. Under the reduced stress conditions, MNS works to suppress the geometric distortion of fine blanking punches.

Let us consider the relationship between the tool steel punch matrix and the surface treatment. When using the PVD coating, its coated punch is subjected to high stress concentration by metal flow with the singularity at the punch edges. Even if the coating layer had sufficient stiffness not to initiate the cracks, the substrate could plastically deform and induce the onset of failure. The coating thickness is still lower than the affected zone thickness by stress concentration. On the other hand, the heat treated layer has enough thickness more than this affected zone depth, but its hardness is insufficient to preserve the integrity against the abrasive wear. MNSed layer thickness reached 40  $\mu\text{m}$ , more than the affected zone thickness. Its average hardness reached 1400 HV against the abrasive wear.

In the ordinary nitriding process [14], the punch surface layer is hardened by fine nitride precipitates. The plasma nitrided tools at relatively high holding temperature have a risk of punch edge embrittlement. The coarsened nitride precipitates have a risk to trigger the fatigue cracking under the high stress transients with increasing N. In the MNS, no nitrided are synthesized as a precipitate to drive the punch-edge embrittlement and fatigue cracking. As reported in [15], MNSed punch surface has chemical inertness enough to be from adhesive wear from the work materials.

Different from the coating method [11], the initial clearance and punch edge profile were preserved after MNS treatment. As shown in Fig. 8, the hardened layer was formed from the original surface to the depth of punch. Although the surface roughness might be induced by crystalline lattice expansion of SKH51 via the MNS process [7, 8, 16], the initial punch surface remains as it was. In its hardness depth profile, the homogeneous hardness plateau with the average of 1400 HV gradually decreases to the matrix hardness of SKH51 with the depth. There was no risk of inner fatigue crack initiation and failure damage. The inner SKH51 matrix was constrained by this hardened surface layer against the applied stresses and displacements.

## Summary

The optimum chamfering technique with massive nitrogen supersaturation treatment plays a synergetic role to reduce the geometric distortion of punch profiles, to improve the blank quality and to make tool life extension. In particular, the lateral and axial displacements of edges and edge-corners were suppressed and saturated to several micro-meters or less than 10% of clearance even until  $N = 50$ . This results promises that this punch design should be applicable to practical fine blanking processes to yield the net-shaped parts and mechanical elements.

## References

- [1] K. Lange, F. Birzer, P. Hofel, A. Munkhoty, H. Singer, Cold Forming and Fineblanking, (1997) 5.
- [2] Q. Zheng, X. Zhuang, Z. Zhao, State-of-the-art and future challenge in fine-blanking technology. *Production Engineering*. 13 (2018) 61-70.
- [3] R. G. Balijepalli, M. R. Begley, N. A. Fleck, R. M. McMeeking, E. Arzt, Numerical simulation of the edge stress singularity and the adhesion strength for compliant mushroom fibrils adhered to rigid substrates. *Int. J. Solid Structures*. 85-86 (2016) 160-171.
- [4] K. Fuchiwaki, M. Takeshita, Y. Matsumoto, T. Aizawa, Fine blanking punch edge control for life extension. *Proc. JSTP* (2021) 602.
- [5] K. Fuchiwaki, T. Aizawa, Enhancement of punch tool life in fine blanking by massive nitrogen supersaturation treatment. *Proc. AWMFT and APSTP 2025* (2025, November; Kaohsiung, Taiwan) 211-212.

- 
- [6] K. Fuchiwaki, T. Aizawa, Punch edge control for tool life extension and finer blanking. *Mater. Trans.* (2026) (in press).
- [7] A-R. Farghali, T. Aizawa, Nitrogen supersaturation process in the AISI420 martensitic stainless steels by low temperature plasma nitriding. *ISIJ International* 58 (3) (2018) 401-407.
- [8] T. Aizawa, Low temperature plasma nitriding of austenitic stainless steels. Chapter 3 in *Stainless steels and alloys*. IntechOpen, London, UK (2019) 31–50.
- [9] T. Aizawa, Micro-/meso-structure control of multi-hostmetal alloys by massive nitrogen supersaturation. *Materials* 17, 1294 (2024) 1-13.
- [10] Y. Suzuki, T. Shiratori, M. Murakawa, M. Yang, Precision stamping process of metal micro gears. *Procedia Manufacturing* 15 (2018) 1445-1451.
- [11] T. Kashi, N. Horikawa, T. Miyajima, A. Ueno, A. Sakaida, Y. Kawano, Y. Yamamoto, Fatigue strength of high-speed tool steel, JIS SKH51 with TiAlN/DLC nano-multilayered hard coating film. *J. Jpn. Soc. Design Eng.* 53 (1) (2018) 43-56.
- [12] G. Claus, M. Weber, M. Demmler, Increase of lifetime for fine blanking tools. *Procedia Eng.* 183 (2017) 45-52.
- [13] M. Sahli, X. Roizard, G. Colas, M. Assoul, L. Carpentier, P-H. Cornuault, S. Giampiccolo, J. P. Barbe, Modelling and numerical simulation of steel sheet fine blanking process. *Procedia Manufacturing* 50 (2020) 395-400.
- [14] A. G. F. Araújo, M. Naeem, L. N. M. Araújo, T. H. C. Costa, K. H. Khan, J. C. Díaz-Guillén, J. Iqbal, M. S. Liborio, R. R. M. Sousa, Design, manufacturing and plasma nitriding of AISI-M2 steel forming tool and its performance analysis. *J. Mater. Res. Technol.* 9 (6) (2020) 14517-14527.
- [15] K. Dohda, M. Yamamoto, C. Hu, L. Dubar, K. F. Ehmman, Falling phenomena in metal forming. *Friction* 9 (2021) 665-685.
- [16] A-R. Farghali, T. Aizawa, T. Yoshino, Microstructure/mechanical characterization of plasma nitrided fine-grain austenitic stainless steels at low temperature. *J. Nitrogen* 2 (2) (2021) 244-258.